© 2016. Published by The Company of Biologists Ltd | Journal of Cell Science (2016) 129, 4521-4533 doi:10.1242/jcs.194738

RESEARCH ARTICLE

Perturbations in actin dynamics reconfigure protein complexes that modulate GCN2 activity and promote an eIF2 response

Richard C. Silva[1,‡], Evelyn Sattlegger[2] and Beatriz A. Castilho[1,*]

ABSTRACT

Genetic and pharmacological interventions in yeast and mammalian cells have suggested a cross-talk between the actin cytoskeleton and protein synthesis. Regulation of the activity of the translation initiation factor 2 (eIF2) is a paramount mechanism for cells to rapidly adjust the rate of protein synthesis and to trigger reprogramming of gene expression in response to internal and external cues. Here, we show that disruption of F-actin in mammalian cells inhibits translation in a GCN2-dependent manner, correlating with increased levels of uncharged tRNA. GCN2 activation increased phosphorylation of its substrate eIF2α and the induction of the integrated stress response master regulator, ATF4. GCN2 activation by latrunculin-B is dependent on GCN1 and inhibited by IMPACT. Our data suggest that GCN2 occurs in two different complexes, GCN2–eEF1A and GCN2–GCN1. Depolymerization of F-actin shifts GCN2 to favor the complex with GCN1, concomitant with GCN1 being released from its binding to IMPACT, which is sequestered by G-actin. These events might further contribute to GCN2 activation. Our findings indicate that GCN2 is an important sensor of the state of the actin cytoskeleton.

KEY WORDS: Translation initiation, GCN2, Actin, GCN1, EEF1A, IMPACT

INTRODUCTION

Protein synthesis regulation modulates a variety of processes in eukaryotes. One key mechanism for regulating global translation is the phosphorylation of eukaryotic translation initiation factor eIF2 (Sonenberg and Hinnebusch, 2009). The heterotrimeric eIF2 factor, associated with GTP, delivers the initiator methionyl-tRNAi^{Met} to the 40S ribosomal subunit at each round of translation initiation, after which it is released as eIF2–GDP. A wide range of stress conditions lead to the phosphorylation of the alpha subunit of eIF2 on Ser^{51} in *Saccharomyces cerevisiae* and mammals, or in a corresponding residue in other eukaryotes. This phosphorylation converts eIF2 from a substrate to an inhibitor of its own guanine nucleotide exchange factor eIF2B, leading to attenuation of general protein synthesis (Hinnebusch, 2014). Paradoxically, the resulting reduction in eIF2 activity stimulates translation of select mRNAs such as those encoding Gcn4 in yeast, and ATF4 (CREB2) and CHOP in mammals, which play key roles in the general amino acid control (GAAC) or the integrated stress response (ISR), in yeast and mammals, respectively. This pathway activates a protective gene expression program that enables cells to recover from the initial stress that triggered it (Baird and Wek, 2012; Harding et al., 2000; Hinnebusch, 2005; Vattem and Wek, 2004).

There are four known eIF2 kinases in mammals (reviewed in Dever, 2002; Donnelly et al., 2013): PERK (encoded by *EIF2AK3*), activated in response to the accumulation of misfolded proteins in the endoplasmic reticulum; PKR (encoded by *EIF2AK2*), activated by double-stranded RNA; HRI (encoded by *EIF2AK1*), by hemin deprivation; and GCN2 (encoded by *EIF2AK4*), activated in response to suboptimal levels of amino acid, serum, or glucose, and also by UV irradiation and proteasome inhibition, to name just a few activation triggers. GCN2 is present in virtually all eukaryotes and is the only eIF2α kinase in *S. cerevisiae*, where it has been extensively studied (reviewed in Castilho et al., 2014; Hinnebusch, 2005).

GCN2 is an important sensor of amino acid availability. Under nutrient-replete conditions it is kept in a latent state by several auto-inhibitory interactions (Garriz et al., 2009; Lageix et al., 2015). Uncharged tRNA that accumulates under amino acid depletion or other stress conditions binds to a region in GCN2 with homology to histidyl tRNA synthetases (HisRS). This results in allosteric rearrangements in GCN2 that lead to its autophosphorylation at a threonine residue in the activation loop of the kinase domain, allowing GCN2 to efficiently bind and phosphorylate its substrate, eIF2α. At the GCN2 amino terminus, the RWD domain (from its presence in RING finger proteins, WD-repeat-containing proteins and DEAD-like helicases) binds directly to the effector protein GCN1, an interaction that is essential for GCN2 activation *in vivo* but not for the kinase activity per se (Marton et al., 1993; Sattlegger and Hinnebusch, 2000). GCN1 is believed to be involved in the transfer of uncharged tRNAs from the ribosomal A site to the HisRS domain of GCN2, when both proteins are bound to translating ribosomes (Marton et al., 1997; Sattlegger and Hinnebusch, 2000). In mammals, GCN2 also regulates synaptic plasticity and memory formation, feeding behavior, cell cycle control, the sensing of intracellular bacterial invasion, and has been implicated in diseases such as cancer and Alzheimer's (reviewed in Castilho et al., 2014; Donnelly et al., 2013).

Other proteins have been reported to modulate GCN2 activity and/or activation, implying that a complex network has evolved to tightly control its function (Castilho et al., 2014). One such protein in yeast, Yih1 and its mammalian ortholog, IMPACT, contain an RWD domain that shares similarities with the RWD domain of GCN2. Like GCN2, Yih1/IMPACT also binds to GCN1, and this leads to reduced GCN1–GCN2 interaction in yeast and mammalian cells (Cambiaghi et al., 2014; Sattlegger et al., 2004). Overexpression of Yih1/IMPACT in yeast and mouse embryonic fibroblasts (MEFs) impairs GCN2 activation under different stress conditions (Cambiaghi et al., 2014; Pereira et al., 2005; Sattlegger

[1]Department of Microbiology, Immunology and Parasitology, Escola Paulista de Medicina, Universidade Federal de São Paulo, São Paulo 04023-062, Brazil. [2]Institute of Natural and Mathematical Sciences, Massey University, Auckland 0745, New Zealand.
‡Present address: Department of Mechanistic Cell Biology, Max Planck Institute of Molecular Physiology, Dortmund 44227, Germany.

*Author for correspondence (bacastilho@unifesp.br)

B.A.C., 0000-0003-4509-5237

Received 18 July 2016; Accepted 31 October 2016

Journal of Cell Science (2016) 129, 4521-4533 doi:10.1242/jcs.194738

et al., 2004). Depletion of IMPACT in neuron-like N2a cells, which express high levels of IMPACT in comparison with MEFs, leads to a higher basal level of GCN2 activity and to a stronger GCN2 activation under leucine deprivation (Roffe et al., 2013). Taken together, these data indicate that Yih1/IMPACT competitively inhibits the GCN1-mediated activation of GCN2. Yih1 also binds to G-actin, as determined by the isolation of this heterodimeric complex by size-exclusion chromatography and velocity sedimentation assays (Sattlegger et al., 2004). IMPACT expressed in yeast interacts with actin, suggesting that IMPACT/Yih1–actin interaction is conserved (Waller et al., 2012).

In yeast, the eukaryotic elongation factor 1A (eEF1A), which delivers aminoacyl-tRNAs to ribosomes during the elongation step of protein synthesis, associates directly with the GCN2 C-terminal domain (Visweswaraiah et al., 2011). Interestingly, *in vivo*, eEF1A–GCN2 complex formation is found under replete but not amino acid starvation conditions. Furthermore, *in vitro*, eEF1A inhibits GCN2 phosphorylation of eIF2α without repressing GCN2 autophosphorylation activity. Together with the fact that *in vitro*, uncharged tRNA displaces eEF1A from GCN2, it was then proposed that eEF1A contributes to keeping GCN2 in its latent state under nutrient-replete conditions. It could do this by either impeding the binding of GCN2 to its substrate, eIF2α, or by preventing the complete intramolecular rearrangements of GCN2 required for the phosphorylation of eIF2α (Visweswaraiah et al., 2011). eEF1A binds to F-actin (Liu et al., 1996; Munshi et al., 2001), and in yeast, mutations in eEF1A that affect aminoacyl-tRNA binding simultaneously cause actin binding and/or bundling defects and increased phosphorylation of eIF2α dependent on GCN2 (Gross and Kinzy, 2007; Perez and Kinzy, 2014).

Polysomes, mRNAs, eukaryotic initiation factors, elongation factors and aminoacyl-tRNA synthetases associate with actin, suggesting that the actin cytoskeleton acts as an organizational scaffold for components of the translational machinery and as a mechanism for localized translation (Bektaş et al., 1994; Dang et al., 1983; Furukawa et al., 2001; Howe and Hershey, 1984; Kelly et al., 2007; Kim and Coulombe, 2010; Sattlegger et al., 2014; Sotelo-Silveira et al., 2008). Evidence for the role of actin in regulating protein synthesis comes from diverse sources. In mammalian cells, disruption of F-actin prevents recovery from a translational block elicited by different stress conditions (Stapulionis et al., 1997). In yeast, protein synthesis requires an intact F-actin cytoskeleton (Gross and Kinzy, 2007). Molecular mechanisms linking the modulation of global protein synthesis to the integrity of the actin cytoskeleton are still poorly understood. Recent reports have indicated that G-actin promotes the stabilization of the complex between phosphatase PP1 and its regulatory subunits, the inducible PPP1R15A (GADD34) or the constitutive PPP1R15B (CReP), that provide the exquisite specificity of this complex towards phosphorylated eIF2α (P-eIF2α) (Chambers et al., 2015; Chen et al., 2015).

Here, we show that the depolymerization of F-actin in mammalian cells elicits a GCN2-mediated eIF2α phosphorylation response, with attenuation of global translation and an increase in ATF4 and CHOP expression. An increased G-actin:F-actin ratio promotes the displacement of eEF1A from GCN2 and of GCN1 from IMPACT, which is drawn to a complex with G-actin. These events coincide with increased association between GCN2 and its effector protein GCN1. Disruption of F-actin also results in the accumulation of deacylated tRNAs, which combined with the reorganization of those complexes, might contribute to the activation of GCN2.

RESULTS

Disruption of F-actin in mouse embryonic fibroblasts triggers a GCN2-mediated eIF2α phosphorylation response

In order to determine if perturbations in actin dynamics could elicit a GCN2 response, mouse embryonic fibroblasts (MEFs) were treated with latrunculin-B, an agent that disrupts the actin cytoskeleton by occupying the ATP-binding pocket in monomeric G-actin, thus preventing actin polymerization (Spector et al., 1989). GCN2 was promptly activated in MEFs following 30 min of treatment with latrunculin-B, as judged by immunoblots with antibodies against the phosphorylated Thr^{898} residue (P-GCN2). Phosphorylation of eIF2α was induced in *Gcn2*$^{+/+}$ cells by latrunculin-B (Fig. 1A). This was a result of specific activation of GCN2, as no significant increase in P-eIF2α was detected in *Gcn2*$^{-/-}$ MEFs subjected to the same treatment (Fig. 1A). Phosphorylation of eIF2α increases the translation of the transcriptional activator ATF4 and of CHOP, encoded by a gene that is transcriptionally upregulated by ATF4, and itself translationally upregulated by increased P-eIF2α (Young et al., 2015). As expected, the expression of both proteins increased in *Gcn2*$^{+/+}$ MEFs, but not in *Gcn2*$^{-/-}$ cells (Fig. 1A). Interestingly, the signal for P-GCN2 persisted for only 1 h, returning rapidly to basal levels by 2 h. By contrast, the phosphorylation of eIF2α increased up to the last time point analyzed (Fig. 1A).

We then treated MEFs with cytochalasin-D, a drug that caps the growing barbed end of F-actin, preventing its polymerization by a mechanism that largely differs from the one exerted by latrunculin-B (Spector et al., 1989). Cytochalasin-D also activated GCN2 and promoted an increase in P-eIF2α levels (Fig. 1B), resulting in increased expression of ATF4 and CHOP (Fig. S1A). Similarly to the response elicited by latrunculin-B, GCN2 was rapidly activated within 30 min of addition of cytochalasin-D. The phosphorylated GCN2 persisted for longer in comparison with latrunculin-B treatment, but decreased considerably by 3 h (Fig. 1B). The ratio of P-eIF2α/eIF2α relative to the untreated control was also slightly higher for cytochalasin-D than for latrunculin-B. As found for latrunculin-B, cytochalasin-D did not promote eIF2α phosphorylation in *Gcn2*$^{-/-}$ MEFs, further indicating that GCN2 is the only eIF2 kinase activated in response to F-actin depolymerization (Fig. 1B). By contrast, the promotion of polymerization and stabilization of actin filaments by jasplakinolide had no detectable effect on the activation of GCN2 and did not promote an increase in P-eIF2α (Fig. 1C) or in ATF4 expression (Fig. S1A).

For comparative purposes, cells were subjected to leucine starvation (Fig. 1D). The extent of GCN2 activation elicited by amino acid starvation was initially slightly lower than that observed by F-actin disassembly. At later times of leucine starvation P-GCN2 levels continued to increase and remained high, as expected, in contrast to the actin depolymerizing conditions where P-GCN2 abruptly decreased as commented above.

To ascertain that the drugs affected the F-actin content in these experiments, *Gcn2*$^{+/+}$ MEFs treated with the aforementioned drugs were stained with FITC-conjugated phalloidin, which binds to F-actin, and analyzed by flow cytometry. By 30 min of treatment, MEFs presented a reduction in F-actin of ∼28% (latrunculin-B) or 48% (cytochalasin-D) in relation to vehicle (DMSO)-treated cells (Fig. 2A,B). These observations correlate with the extent of activation of GCN2 detected by 30 min of action of these drugs. The amount of F-actin in MEFs treated with either drug gradually dropped along the time points analyzed, with cytochalasin-D-treated cells maintaining a more pronounced reduction. Interestingly, at the time points when GCN2 phosphorylation

Journal of Cell Science (2016) 129, 4521-4533 doi:10.1242/jcs.194738

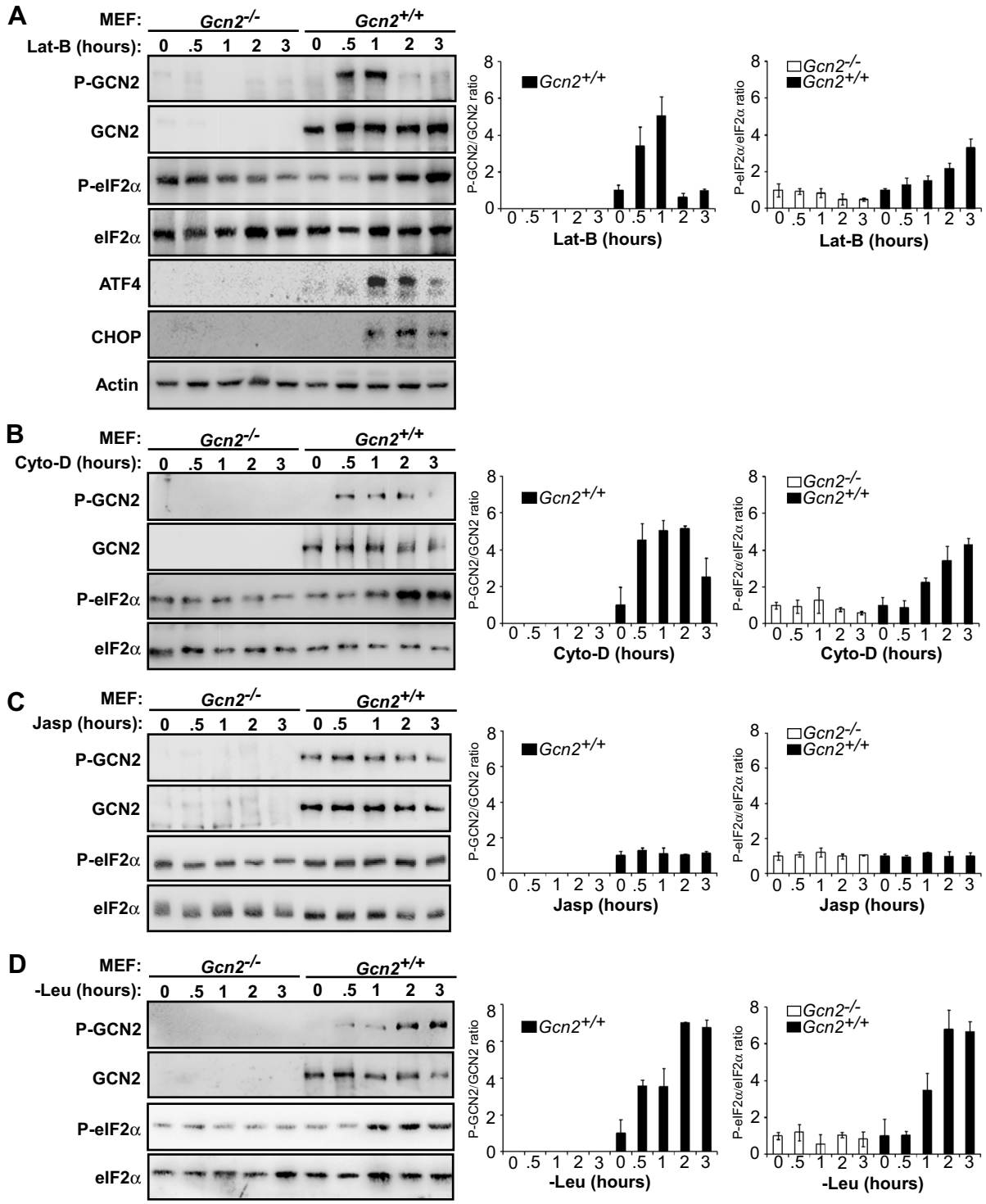

Fig. 1. F-actin disruption induces a GCN2-dependent phosphorylation of eIF2α and upregulation of ATF4 and CHOP. Immunoblots of extracts of *Gcn2*$^{+/+}$ and *Gcn2*$^{-/-}$ MEFs for detection of the indicated proteins and their phosphorylated forms. Cells were treated with (A) latrunculin-B, (B) cytochalasin-D or (C) jasplakinolide, or (D) subjected to leucine starvation, for the indicated times. The respective membranes stained with Ponceau are shown in Fig. S1B. For each condition, a representative result of at least three independent experiments is shown. The ratios of signals for phosphorylated GCN2 or eIF2α relative to the signal for total GCN2 or eIF2α were calculated for each time point and the ratio at time zero was set to 1. Data are presented on the graphs as mean±s.e.m. from at least three independent experiments.

decreased dramatically (2 h with latrunculin-B, and 3 h with cytochalasin-D), actin was clearly depolymerized. The treatment with jasplakinolide was effective, as these cells could not be stained with conjugated phalloidin (data not shown), which shares the same binding site with jasplakinolide on F-actin (Bubb et al., 1994). To better estimate the effect of jasplakinolide, we stained jasplakinolide-treated MEFs with Alexa-Fluor-594-conjugated DNase-I that binds specifically to G-actin (Fig. 2C). The levels of

Journal of Cell Science (2016) 129, 4521-4533 doi:10.1242/jcs.194738

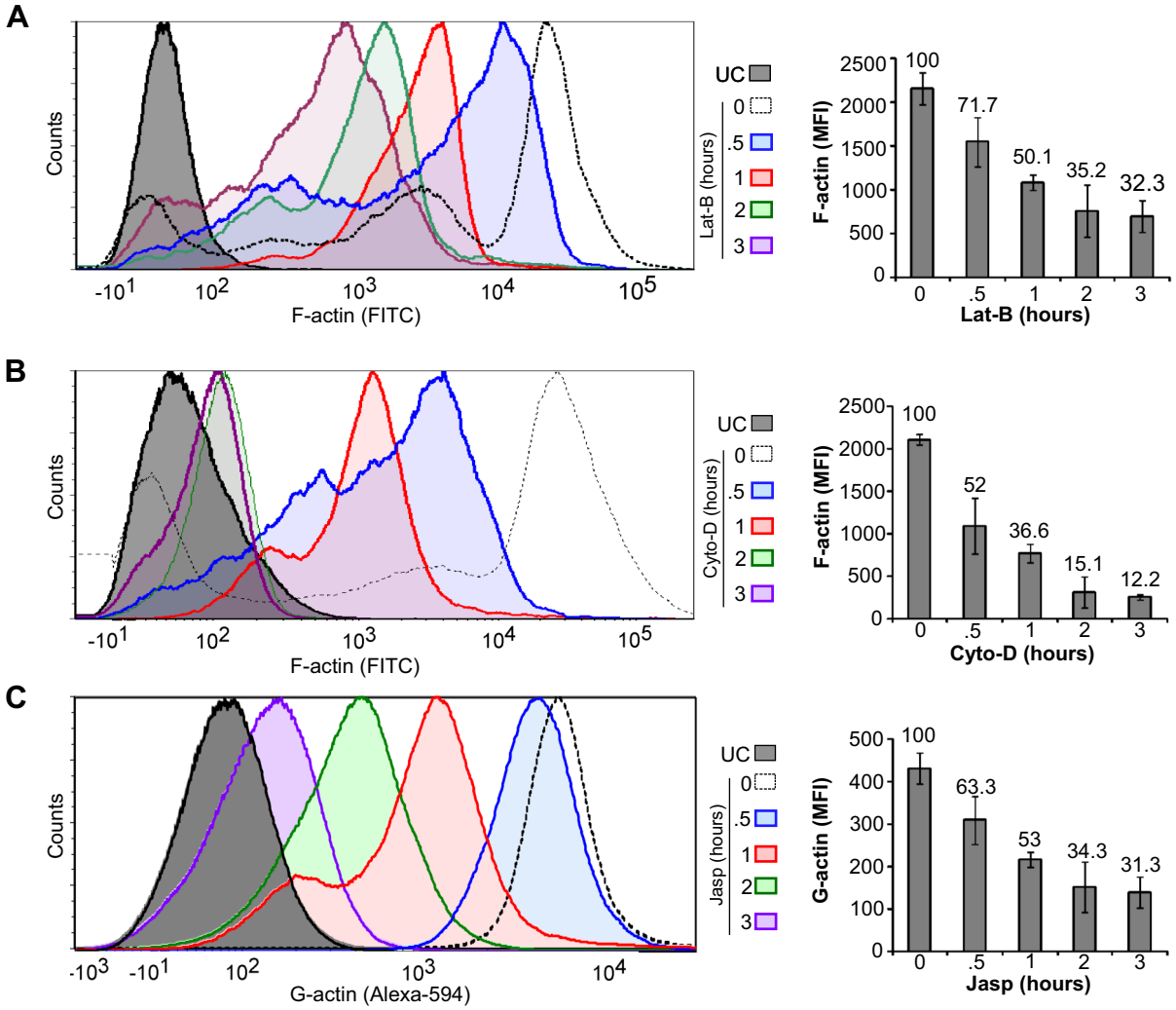

Fig. 2. Effects of drugs on F-actin or G-actin content in MEFs. Representative histograms of flow cytometry analyses of *Gcn2*$^{+/+}$ MEFs treated with (A) latrunculin-B, (B) cytochalasin-D or (C) jasplakinolide for the indicated times. Cells treated with latrunculin-B or cytochalasin-D were stained with phalloidin–FITC. Cells treated with jasplakinolide were stained with DNase-I–Alexa-594. A total of 1×10^4 cells were analyzed per acquisition using the FL1A or FL2A channel. Unstained cells (UC) were used to define the basal fluorescence signal (gray filled histograms). Cells incubated with 0.1% DMSO for 3 h were used as control (untreated cells, 0– black dotted lines). Colors of histograms represent different time points of each treatment, as indicated. Bar graphs on the right represent the mean fluorescence intensities (MFI) of each cell population shown on the left panels, with basal fluorescence of unstained controls subtracted from the values. Numbers above columns represent the percentage of F-actin fluorescence intensity relative to that in vehicle (DMSO)-treated cells (set at 100%). Data represent mean±s.e.m. of three independent experiments performed in duplicate.

G-actin decreased gradually along the time points analyzed, confirming that the jasplakinolide treatment promoted the stabilization of F-actin. Leucine starvation did not affect the F-actin cytoskeleton (Fig. S1C).

Taken together, these data show that the disassembly of F-actin, but not its stabilization, elicits a GCN2-mediated eIF2α phosphorylation response in MEFs, and this is likely the result of an increase in the ratio of G-actin:F-actin.

GCN2 was not activated in MEFs treated with nocodazole, an inhibitor of microtubule polymerization (Fig. S2), indicating that GCN2 senses a signal triggered by actin, but not microtubule, cytoskeleton disruption.

In order to determine whether activation of GCN2 upon disruption of F-actin is a conserved phenomenon, we assessed the eIF2α response in *S. cerevisiae* cells treated with latrunculin-B (Fig. S3). Interestingly, disruption of actin filaments did not lead to significant changes in P-eIF2α levels (Fig. S3A). We also assessed the expression of a reporter consisting of the *GCN4* promoter and sequences encoding its mRNA leader, containing the four upstream open reading frames, fused to *lacZ*. No significant change in β-galactosidase activity was detected in cells treated with latrunculin-B compared with control non-treated cells (Fig. S3B). Latrunculin-B led to depolymerization of F-actin in these cells, as determined by phalloidin-FITC staining (Fig. S3C). These results are in agreement with previous reports that in yeast, latrunculin-B does not result in increased eIF2α phosphorylation and does not affect translation rates (Cameroni et al., 2006; Kandl et al., 2002). Interestingly, however, disassembly of microtubules by nocodazol resulted in a strong phosphorylation of eIF2α in yeast (Fig. S3D).

Activation of GCN2 by actin depolymerization requires GCN1 and is inhibited by IMPACT

The activation of mammalian GCN2 by F-actin depolymerization requires GCN1, as determined by decreasing GCN1 expression with siRNA (Fig. 3A). Although the downregulation of GCN1 expression was not highly efficient, the small decrease in the

Journal of Cell Science (2016) 129, 4521-4533 doi:10.1242/jcs.194738

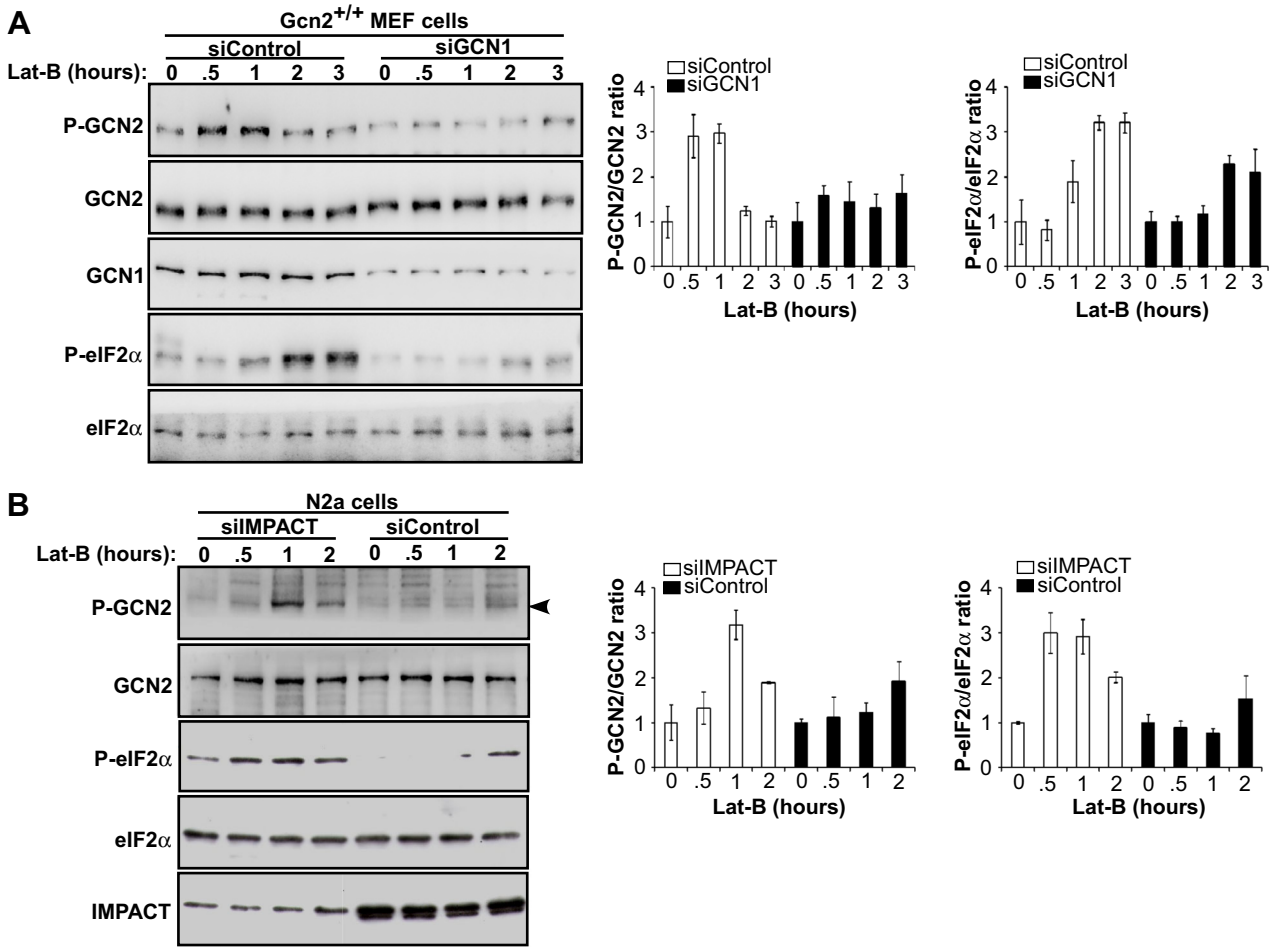

Fig. 3. GCN2 activation by F-actin depolymerization requires GCN1 and is inhibited by IMPACT. (A) *Gcn2*$^{+/+}$ MEFs transfected with siGCN1 or with scrambled siRNA (siControl) or (B) undifferentiated N2a cells transfected with siIMPACT or with siControl were incubated in medium containing latrunculin-B for the indicated times. Cell extracts were used in immunoblots to detect the indicated proteins and their respective phosphorylated forms. Note: in this particular blot, IMPACT is observed as a duplet band. The figures are a representative of three independent experiments. The ratios of signals for phosphorylated GCN2 or eIF2α relative to the signal for total GCN2 or eIF2α were calculated for each time point and the ratio at time zero was set to 1. Data are presented in the graphs as mean±s.e.m. from at least three independent experiments.

abundance of GCN1 was sufficient to clearly lower the activation of GCN2 and eIF2α phosphorylation in cells treated with latrunculin-B compared with cells transfected with control siRNA. As expected, GCN1 downregulation inhibited GCN2 activation when cells were starved of leucine (Fig. S4).

Next, we addressed whether IMPACT inhibits GCN2 activation in the context of F-actin disruption. Here, we made use of murine-neuronal-like N2a cells, which express larger amounts of endogenous IMPACT compared with MEFs (Roffe et al., 2013). N2a cells were transfected with siRNA against IMPACT or with a control siRNA and then subjected to latrunculin-B treatment (Fig. 3B). Depletion of IMPACT resulted in stronger activation of GCN2 compared with cells transfected with siControl in response to latrunculin-B. In N2a cells, the levels of P-GCN2 showed a strong decrease after the initial activation, just as observed for MEFs.

Our results then show that GCN2 activation triggered by depolymerization of F-actin requires GCN1, and that IMPACT suppresses the activity of GCN2 as expected for its proposed function as a competitor of GCN2 for the binding to GCN1. These data also demonstrated that F-actin disruption elicits the activation of GCN2 in different cell types.

Disruption of F-actin mediates a GCN2-dependent inhibition of global protein synthesis and reduces amino acylated tRNA levels

In light of the results shown above, we revisited previous accounts that protein synthesis is affected by the state of the actin cytoskeleton (Stapulionis et al., 1997). Protein synthesis was monitored by immunoblots of extracts of cells treated with puromycin, a structural analogue of aminoacyl-transfer RNA that is incorporated into nascent polypeptide chains causing premature termination, using anti-puromycin antibodies (Schmidt et al., 2009) (Fig. 4A). This assay was highly specific as strong labeling was obtained for cells incubated with puromycin, whereas pre-treatment of *Gcn2*$^{+/+}$ MEFs with cycloheximide fully abrogated incorporation of puromycin, implying that only nascent polypeptides were labeled (Fig. 4A). Steady state levels of actin, determined by incubation of the same membranes with anti-actin antibodies, were used as loading control. Next, puromycin was added to *Gcn2*$^{+/+}$ and *Gcn2*$^{-/-}$ MEFs previously exposed to latrunculin-B for 1 h (Fig. 4B), or subjected to leucine withdrawal for 3 h for comparison (Fig. 4C). Quantification of the signals is shown in Fig. 4D. As anticipated from the increased levels of GCN2-mediated eIF2α phosphorylation induced by latrunculin-B (Fig. 1A), there was a decrease in protein synthesis

Journal of Cell Science (2016) 129, 4521-4533 doi:10.1242/jcs.194738

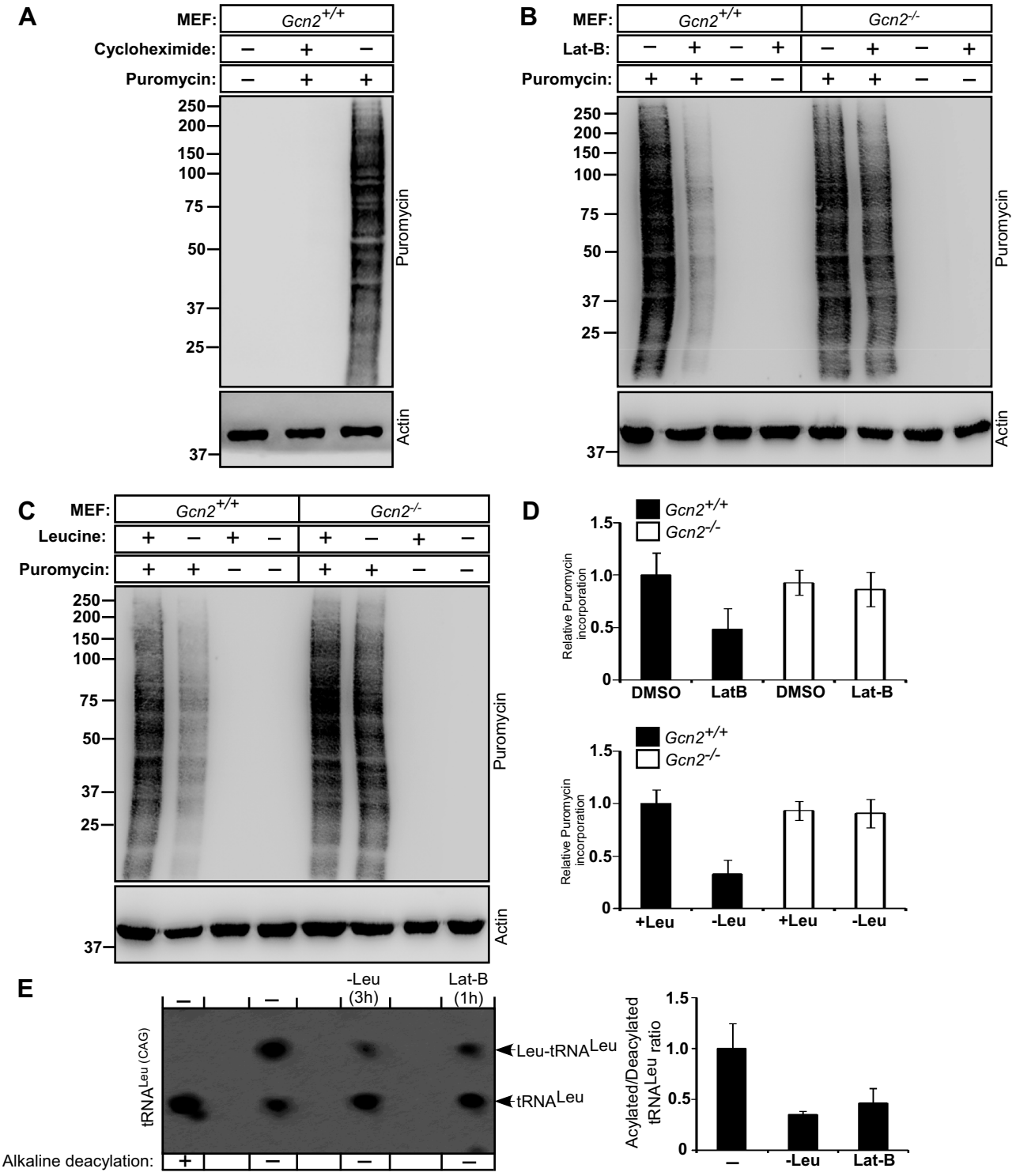

Fig. 4. Translation attenuation in response to F-actin disruption is dependent on GCN2. *Gcn2*$^{+/+}$ and *Gcn2*$^{-/-}$ MEFs were incubated in medium supplemented (+) or not (–) with puromycin for 10 min prior to harvesting. Proteins were subjected to immunoblot with anti-puromycin antibodies and, after striping, with anti-actin antibodies. Molecular mass markers are shown in kDa. (A) *Gcn2*$^{+/+}$ MEFs grown under normal conditions were treated (+) or not (–) with 25 µM cycloheximide for 5 min and processed as above. (B) *Gcn2*$^{+/+}$ and *Gcn2*$^{-/-}$ MEFs were incubated with latrunculin-B or with DMSO for 1 h. (C) *Gcn2*$^{+/+}$ and *Gcn2*$^{-/-}$ MEFs were incubated in medium with or without leucine for 3 h, as indicated. (D) Bar graphs depict the relative intensity of lanes 1, 2, 5 and 6 from immunoblots shown in B and C. The intensity of lane 1 was set to 1. Data are presented as mean±s.e.m. from three independent experiments. (E) Representative northern blot hybridized with a probe to detect tRNA^{Leu}. Bulk RNA extracted under acidic conditions from *Gcn2*$^{+/+}$ MEFs subjected to latrunculin-B treatment for 1 h, leucine starvation for 3 h, or left untreated, was separated by acid-denaturing RNA-PAGE in alternate lanes. Charged (Leu-tRNA^{Leu}) and uncharged (tRNA^{Leu}) forms of the tRNA were detected with a biotin-labeled oligonucleotide probe against tRNA^{Leu} (CAG). As a control, RNAs were deacylated under alkaline conditions prior to the northern analysis. Bar graph on the right depicts relative tRNA charging levels are presented as the ratio of uncharged to aminoacylated tRNA, relative to the same ratio in untreated cells, as determined by quantification of two independent experiments using ImageJ. Charging ratio of untreated cells was set to 1. Error bars indicate s.e.m.

Journal of Cell Science (2016) 129, 4521-4533 doi:10.1242/jcs.194738

in wild-type MEFs with an ~50% reduction after 1 h of latrunculin-B treatment (Fig. 4B,D top panel). In contrast, protein synthesis in *Gcn2*$^{-/-}$ MEFs subjected to the same treatment did not significantly change in relation to cells incubated with DMSO (Fig. 4B,D top panel). Inhibition of translation (reduction of 60%) was observed in MEFs subjected to leucine deprivation for 3 h (Fig. 4C,D bottom panel), and as expected, this effect was dependent on GCN2 (Fig. 4C,D bottom panel). These results then allowed us to conclude that GCN2 activity, likely through the phosphorylation of eIF2α, is required and sufficient for reducing global translation in response to F-actin disruption.

Since deacylated tRNA is the direct signal that triggers the activation of GCN2, we then analyzed tRNA aminoacylation in cells treated with latrunculin-B. RNAs were extracted under acidic conditions from MEFs exposed to latrunculin-B for 1 h, or starved of leucine for 3 h, and tRNA^{Leu} detected by northern blot (Fig. 4E). As a control, RNAs extracted from untreated MEFs were deacylated under alkaline conditions. In cells grown under normal conditions, the majority of the tRNA^{Leu} population was aminoacylated, whereas in cells subjected to leucine depletion for 3 h, the majority of tRNA^{Leu} was deacylated (Fig. 4E). Importantly, in latrunculin-B-treated cells, we observed a substantial increase in the amount of uncharged tRNA^{Leu} and a concomitant decrease in the aminoacylated tRNA^{Leu} relative to untreated cells (Fig. 4E). There was no detectable change in total tRNA^{Leu} levels. These results indicate that depolymerizarion of F-actin affects the aminoacylation of tRNA^{Leu}, and might explain the activation of GCN2 elicited by latrunculin-B treatment.

F-actin depolymerization displaces eEF1A from GCN2 and IMPACT from GCN1, and concomitantly increases GCN2–GCN1 and IMPACT–actin complex formation

Given the observation that GCN2 activation elicited by F-actin depolymerization did not directly correlate with the observed levels of eIF2α phosphorylation, differing in the kinetics observed by amino acid starvation, we then asked whether eEF1A could be involved in these divergent results.

First, in order to determine whether eEF1A binds to GCN2 in mammalian cells, we conducted co-immunoprecipitation experiments. As described for yeast, in MEFs under normal growth conditions, eEF1A was found in association with GCN2, when using anti-eEF1A antibodies for the co-immunoprecitation assays (Fig. 5A, B). Moreover, anti-eEF1A antibodies readily co-precipitated actin, in line with previous reports (Edmonds et al., 1996; Liu et al., 2002). No GCN1 was detected in this complex, similar to what was described for yeast cells (Visweswaraiah et al., 2011). We then performed the reverse immunoprecipitation, using antibodies against GCN2. eEF1A co-precipitated with GCN2, unambiguously indicating that eEF1A forms a complex with GCN2 in mammalian cells (Fig. 5C,D). In this case, however, GCN1 was clearly detected in association with GCN2. Anti-GCN2 antibodies did not co-prepicipitate actin (Fig. 5C,D). Attesting to the specificity of these assays, GAPDH, an abundant protein, did not co-precipitate with either eEF1A or GCN2 (Fig. 5). These results thus indicate that GCN2 forms two different complexes: one with eEF1A, lacking GCN1 (dubbed here Complex GE for GCN2 and eEF1A), and another with GCN1, lacking eEF1A (dubbed here Complex GG, for GCN2 and GCN1) (Fig. 7). They also indicate that the fraction of eEF1A that binds to GCN2 is not associated with the actin cytoskeleton.

If the binding of eEF1A to GCN2 is abrogated by increased levels of uncharged tRNAs, as proposed from *in vitro* experiments and from co-immunoprecipitation data of yeast cells subjected to amino acid starvation (Visweswaraiah et al., 2011), one would expect that leucine starvation in mammalian cells would lead to reduced eEF1A–GCN2 interaction. After 3 h of leucine starvation, eEF1A co-precipitated GCN2 to the same extent as in control cells (Fig. 5A). Also, under the same conditions, GCN2 co-precipitated eEF1A to the same extent as in control cells (Fig. 5C). It is possible that the GCN2–eEF1A uncoupling occurs in a very small percentage of the complexes, undetectable by this assay. To effectively detect eEF1A displacement from GCN2, a longer period of starvation might be necessary, when uncharged tRNAs accumulate to greater levels. Indeed, the yeast data was obtained under a strong amino acid starvation condition induced with sulfometuron (Visweswaraiah et al., 2011). Another possibility is that in mammalian cells, uncharged tRNAs do not promote the separation of eEF1A from GCN2.

Interestingly, though, upon depolymerization of F-actin, a strong decrease in the interaction of eEF1A with GCN2 was clearly evident, in both immunoprecipitation experiments (Fig. 5B,D). F-actin depolymerization also reduced the interaction of eEF1A with actin, as expected (Fig. 5B). Surprisingly, actin depolymerization resulted in an increase in the GCN2 bound to GCN1 (Complex GG) (Fig. 5D). Thus, at the same time that GCN2 is displaced from eEF1A, GCN2 associates with GCN1. This could in principle lead to a higher sensitivity of GCN2 towards uncharged tRNAs.

We next studied the effect of latrunculin-B treatment on the ability of IMPACT to associate with GCN1 in MEFs (Fig. 6). Under control conditions, anti-IMPACT antibodies co-immunoprecipitated GCN1 as expected (Fig. 6A). Neither GCN2 nor GAPDH co-precipitated with IMPACT, as expected (Fig. 6A). Importantly, latrunculin-B treatment reduced the amount of GCN1 associated with IMPACT. Using anti-GCN1 antibodies, IMPACT co-immunoprecipitated with GCN1 under normal growth conditions and this interaction was drastically reduced upon F-actin depolymerization (Fig. 6B). In contrast, association of GCN2 with GCN1 significantly increased in latrunculin-B-treated cells (Fig. 6B), corroborating the immunoprecipitation assays with GCN2 antibodies (Fig. 5D) and unambiguously indicating that actin depolymerization enhances the association of GCN1 with GCN2.

We then addressed the ability of IMPACT to bind actin. Despite intensive efforts, we could not clearly assess the interaction of native IMPACT with actin in MEFs because of its co-migration with antibody heavy chains in SDS-PAGE. Given that knockdown of endogenous IMPACT in N2a cells resulted in stronger GCN2 activation upon F-actin depolymerization (Fig. 3B), we then studied the interaction of actin with IMPACT–FLAG expressed in the N2a cell line (Fig. 6C). IMPACT clearly associates with actin. Latrunculin-B treatment increased the amount of actin that co-precipitates with IMPACT, suggesting that IMPACT preferentially binds to G-actin (Fig. 6C), as does its yeast ortholog (Sattlegger et al., 2004). Supporting the results obtained in MEFs, association of IMPACT with GCN1 was reduced upon F-actin disruption in N2a cells (Fig. 6C). In light of these findings, it is possible that the increase in G-actin upon latrunculin-B treatment sequesters IMPACT away from GCN1, thus freeing GCN1 to associate with GCN2.

DISCUSSION

In this study we provided evidence that the kinase GCN2 responds to the disruption of the actin cytoskeleton and then promotes an eIF2α-phosphorylation response that includes protein synthesis attenuation and an increase in the expression of ATF4,

Journal of Cell Science (2016) 129, 4521-4533 doi:10.1242/jcs.194738

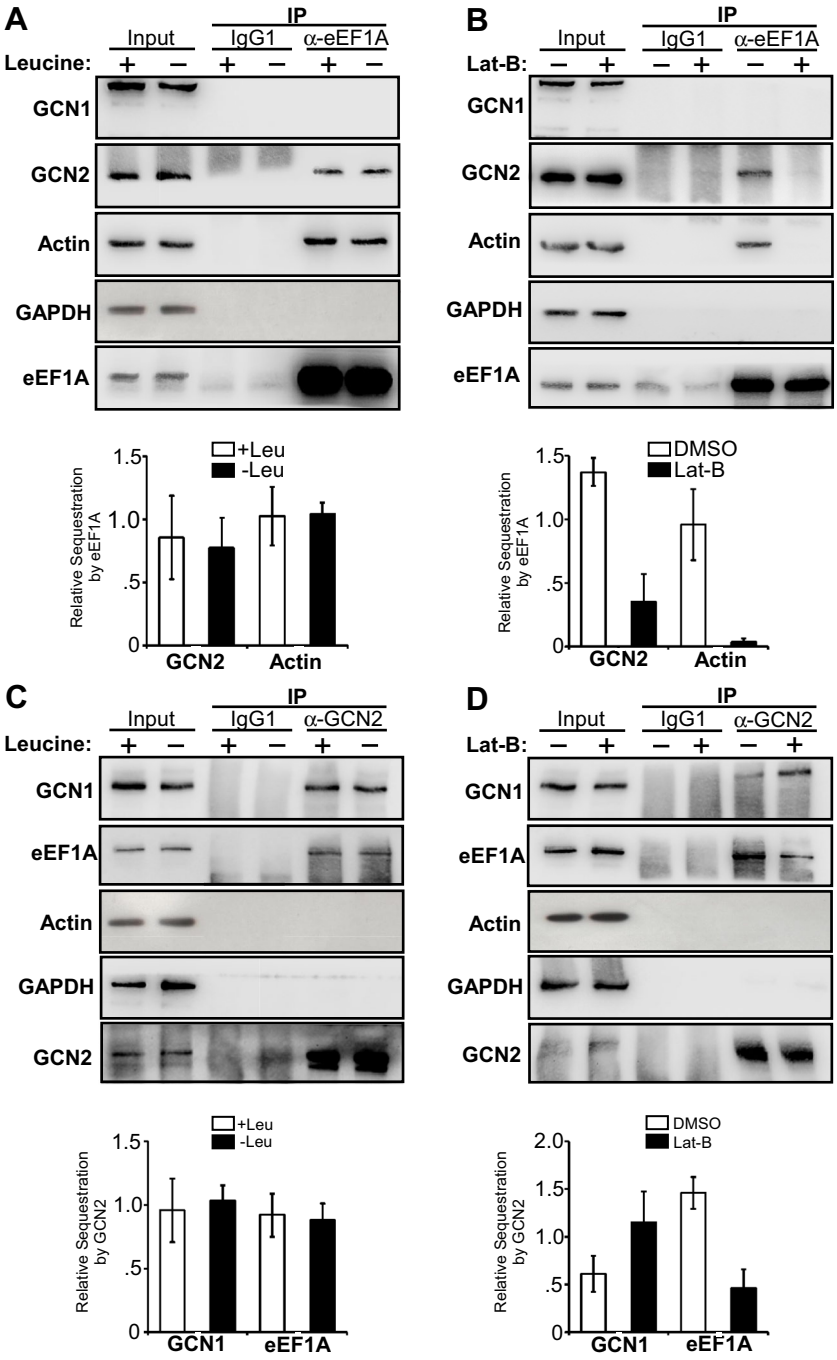

Fig. 5. Actin depolymerization promotes the displacement of eEF1A from GCN2. (A) Extracts from *Gcn2*$^{+/+}$ MEFs incubated in medium lacking leucine for 3 h (−) or in medium containing leucine (+) were used for immunoprecipitation with antibodies against eEF1A or with non-specific antibodies coupled to protein-G agarose beads. Immune complexes and 1% of the input material were separated by SDS-PAGE and analyzed by immunoblot to detect the indicated proteins. (B) *Gcn2*$^{+/+}$ MEFs were incubated in medium containing latrunculin-B (+) or DMSO (−) for 1 h. Cell extracts were used in co-immunoprecipitation assays with anti-eEF1A antibodies as in A. (C) Extracts of MEFs grown as in A were used for immunoprecipitation with anti-GCN2 antibodies bound to protein-G agarose beads. Immune complexes and 1% input were immunoblotted as above. (D) Extracts prepared from MEFs grown as in B were subjected to co-immunoprecipitation using anti-GCN2 antibodies as in C. The amount of proteins sequestered by eEF1A or GCN2 was determined by estimating the amount of precipitated proteins with ImageJ. Values were plotted in a bar graph relative to the values found for their respective inputs. Error bars indicate s.e.m. Data are representative of three to four independent experiments.

the major transcription regulator that allows cells to recover from stress.

Our results show that GCN2 is rapidly activated by exposure of cells to latrunculin-B or cytochalasin-D. Given that these small-molecular-weight metabolites exert their effect through distinct mechanisms that ultimately result in increased levels of free G-actin at the expense of F-actin, activation of GCN2 is most likely a direct result of disruption of the actin cytoskeleton and not a potential side effect exerted by these agents (Spector et al., 1989).

Consistent with our findings that latrunculin-B elicits a GCN2-dependent eIF2α phosphorylation, besides the absence of this response in *Gcn2*$^{-/-}$ cells, is the observed increase in uncharged tRNA^{Leu}, the direct signal for GCN2 activation (Hinnebusch, 2005). Although we did not measure the aminoacylation of other tRNAs, these might also be affected. Disruption of F-actin might hinder the function of amino acid transporters on the plasma membrane, thereby resulting in amino acid starvation, as membrane damage readily elicits amino acid starvation (Tattoli et al., 2012). Additionally, disturbances in the actin cytoskeleton might affect the function of aminoacyl-tRNA synthetases as several of these, including leucyl-tRNA synthetase, are part of a multiprotein complex that interacts with the actin cytoskeleton (Kaminska et al., 2009).

In the latrunculin-B and cytochalasin-D studies, we noticed that the extent of eIF2α phosphorylation relative to that of GCN2 phosphorylation differs from that observed under amino acid starvation conditions. Even though the activation level of GCN2 at 1 h of treatment with the depolymerizing drugs was higher than that observed at 1 h of leucine starvation (5-fold increase in GCN2-P

Journal of Cell Science (2016) 129, 4521-4533 doi:10.1242/jcs.194738

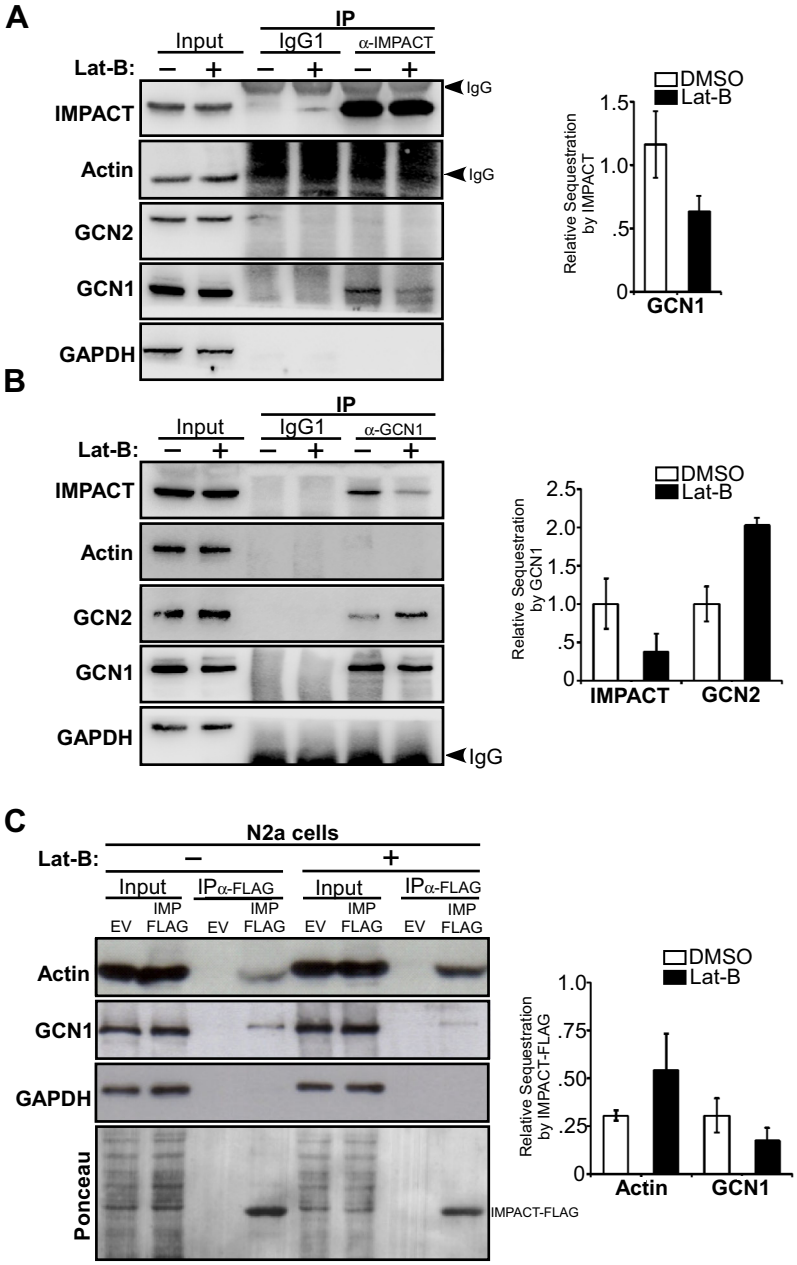

Fig. 6. Actin depolymerization promotes the displacement of IMPACT from GCN1, with the concomitant increase in GCN2–GCN1 complex formation. (A) Extracts of *Gcn2*$^{+/+}$ MEFs treated with latrunculin-B (+) or DMSO (–) for 1 h were used for immunoprecipitation with antibodies against IMPACT or with non-specific antibodies coupled to protein-G agarose beads. Immune complexes and 0.5% of the input material were analyzed by immunoblot to detect the indicated proteins. (B) Extracts as in A were used for immunoprecipitation with anti-GCN1 antibodies. Immune complexes and 1% of the input material were analyzed by immunoblot to detect the indicated proteins. The Ponceau staining of the membrane from a 10% SDS-PAGE is presented in the bottom panel. Black arrowheads in A,B, IgG1 chains. The amount of proteins sequestered by native IMPACT, GCN1 or IMPACT-FLAG was determined by estimating the amount of precipitated proteins with ImageJ. Values were plotted in bar graphs (to the right of each IP plot panel), relative to the values found for their respective inputs. Error bars indicate s.e.m. Data are representative of three (A,B) or two (C) independent experiments.

levels as compared with 3.5-fold, respectively), eIF2α phosphorylation was lower in response to the drugs relative to that elicited by amino acid depletion (1.5–2.0-fold increase versus 3.5-fold, respectively, taking the 1 h time point). These observations can be interpreted in light of recent evidence indicating that monomeric G-actin provides stabilization of the complex between the catalytic subunit of phosphatase 1 (PP1) and its regulatory subunits, the PPP1R15 proteins, and specificity towards P-eIF2α (Chambers et al., 2015; Chen et al., 2015). Indeed, here in *Gcn2*$^{-/-}$ cells, a small decrease in basal P-eIF2α can be detected after latrunculin-B treatment (Fig. 1A) compared with leucine starvation (Fig. 1C), an effect that might be dependent on the constitutive regulatory subunit, PPP1R15B (CReP). In the case of *Gcn2*$^{+/+}$ cells, activation of GCN2 and initial increase of P-eIF2α and thus of ATF4 could induce the transcription and translation of PPP1R1A (GADD34), thus collaborating for the lower levels of eIF2α phosphorylation observed when compared with leucine starvation.

In these previous studies, the authors used jasplakinolide to lower G-actin content, which resulted in increased P-eIF2α (Chambers et al., 2015). In their experiments, latrunculin-B at the same concentration used here did not affect the levels of eIF2α phosphorylation, but increased the association of PP1–PPP1R1 with G-actin. Their interpretation was that G-actin is not rate-limiting for the activity of this phosphatase complex towards eIF2α. Here, we clearly show that latrunculin-B activates GCN2 and increases P-eIF2α, in both MEFs and N2a cells. It should be noted that in the previous studies, the authors added latrunculin-B together with thapsigargin, a strong activator of PERK. It is possible that any increase in P-eIF2α mediated by GCN2 in those studies could have been masked by the phosphorylation of eIF2α by PERK. Another possibility is that differences in culture conditions could explain the discrepancy between our data and that report. The confluency of cell cultures might affect the outcome of the drug treatment. Here, we employed cells at ∼60% confluency when drugs were added. Under

Journal of Cell Science (2016) 129, 4521-4533 doi:10.1242/jcs.194738

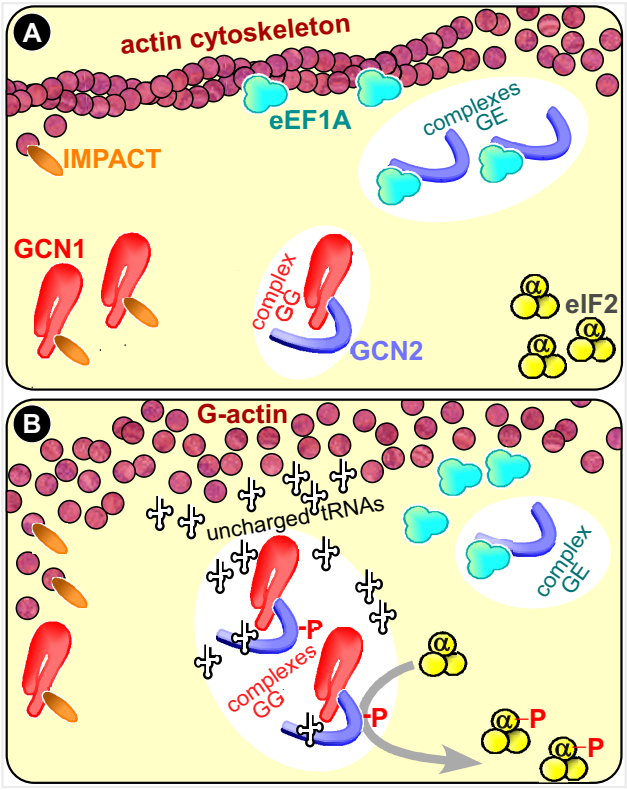

Fig. 7. Model for the activation of GCN2 by F-actin depolymerization. (A) Under normal growth conditions, GCN2 resides mainly in a complex with eEF1A (complex GE) rather than in a complex with GCN1 (complex GG), whereas GCN1 is mainly associated with IMPACT. (B) Under F-actin depolymerization conditions, IMPACT is drawn to a complex with G-actin, liberating GCN1, while GCN2 is also made more available. These events result in more GG complexes where GCN2 is then activated by increased levels of uncharged tRNA. See text for more detail.

these conditions, actin should be in its most plastic state, and therefore more sensitive to the effects of latrunculin-B, compared with confluent cultures. This interpretation might also be valid for the lack of a detectable effect of jasplakinolide in our experiments.

Interestingly, after an initial phosphorylation of GCN2 induced by both latrunculin-B and cytochalasin-D, P-GCN2 levels rapidly decreased (Fig. 1). Considering that F-actin remained low at later time points, as determined by flow cytometry, these results seem to suggest that either P-GCN2 is rapidly degraded whereas the unphosphorylated form is unaffected as no decrease in total GCN2 was detected, or a strong phosphatase acts on P-GCN2. The degradation or dephosphorylation of P-GCN2 might dominate over GCN2 autophosphorylation in response to depolymerized actin at those later times. Either one of these possible events seems to be triggered by F-actin depolymerization as the same phenomenon was not observed under amino acid starvation. It will be important to better understand the molecular basis for this rapid decrease in P-GCN2, which seems to be unique to this stress condition.

Of note was the observation that P-eIF2α levels seemed to increase after the P-GCN2 levels decreased, in both latrunculin-B and cytochalasin-D treatments. It is possible that F-actin depolymerization elicits the activation of yet another eIF2α kinase at later time points. However, this should be dependent on GCN2 activity, as in *Gcn2*$^{-/-}$ cells no phosphorylation of eIF2α is detectable at any point. A more likely possibility is that at the later time points, less PP1–PPP1R15 is present owing to a drastic shutdown of protein synthesis caused by high eIF2α-P levels, which can also affect the translation of PPP1R15A and ATF4. Indeed, the amount of AFT4 drops after a maximum at 1 h of latrunculin-B treatment. Thus, the few remaining activated GCN2 molecules at later time points would have a large effect on the levels of P-eIF2α.

We showed here that GCN2 is found in two complexes, one with GCN1 and another with eEF1A. Amino acid starvation did not alter the abundance of the GCN2–GCN1 complex, similar to observations in yeast (Garcia-Barrio et al., 2000), or the abundance of the GCN2–eEF1A complex. By contrast, depolymerization of F-actin increased GCN2–GCN1 complex formation to the detriment of the GCN2–eEF1A complex. Given that in yeast cells GCN1 is absolutely required for GCN2 activation *in vivo*, and in mammalian cells GCN1 is required, at least, for an efficient GCN2 activation, as shown here, it is likely that GCN2 molecules bound to eEF1A are in a non-activatable state. eEF1A binds to the C-terminal domain of GCN2, whereas GCN1 binds to the extreme N-terminal region of GCN2 (Sattlegger and Hinnebusch, 2000; Visweswaraiah et al., 2011). Thus, although unlikely, it remains to be determined whether the association of GCN1 and eEF1A with GCN2 are mutually exclusive.

eEF1A associates with F-actin and this interaction is conserved across species from yeast to mammals (Gross and Kinzy, 2007; Liu et al., 2002; Munshi et al., 2001). The results shown here are in agreement with those reports, as latrunculin-B treatment abrogated the precipitation of actin with anti-eEF1A antibodies. Our findings suggest that *in vivo*, only the actin-free pool of eEF1A interacts with GCN2.

The signal that triggers the separation of GCN2 from eEF1A, as suggested from the yeast studies, seems to be high levels of uncharged tRNAs (Visweswaraiah et al., 2011). Our data, however, suggest that other mechanisms could also contribute to this uncoupling. This is based on our observations that in cells starved of leucine no change in GCN2–eEF1A complex levels was detected, whereas in cells treated with latrunculin-B, which have slightly fewer uncharged tRNAs compared with leucine-starved cells, GCN2–eEF1A complex levels were reduced. It is possible that this displacement is mediated by free GCN1. An increased ratio of G-actin:F-actin reduced the amount of GCN1 bound to IMPACT. Our data indicate that G-actin could be sequestering IMPACT from its complex with GCN1. Mapping of actin and GCN1 binding sites on Yih1 suggested that they overlap in the central region of Yih1 (Sattlegger et al., 2011). Thus, actin and GCN1 might compete for the binding to Yih1. IMPACT shares a high degree of homology to Yih1, structurally and functionally (Cambiaghi et al., 2014; Pereira et al., 2005; Sattlegger et al., 2011), and the location of the binding sites determined for Yih1 might also apply to IMPACT. The data shown here support the notion that IMPACT might bind either GCN1 or G-actin.

In light of these observations, we propose the model shown in Fig. 7. GCN2 is found in two distinct complexes, GCN2–eEF1A (complex GE) and GCN2–GCN1 (complex GG). GCN1 is also found in two complexes, GCN1–GCN2 (complex GG) and GCN1–IMPACT. Depolymerization of F-actin alters the equilibrium. Increased G-actin levels allow for more G-actin–IMPACT complex formation, thereby making more GCN1 available for binding to GCN2. This, or a parallel independent mechanism, might shift the balance towards decreasing the eEF1A–GCN2 complex. Increased availability of the GCN2–GCN1 complex would sensitize GCN2 more towards its activating ligand – uncharged tRNAs – compared with conditions that do not involve the rearrangements of these complexes. This model could account for the higher levels of P-GCN2 obtained upon actin depolymerization relative to those

Journal of Cell Science (2016) 129, 4521-4533 doi:10.1242/jcs.194738

obtained under leucine starvation even though uncharged tRNAs amounts were slightly lower in the former condition.

Thus, two mechanisms seem to concur for the activation of GCN2 upon the disruption of the F-actin cytoskeleton: (1) uncharged tRNAs activate the GCN2 molecules already complexed with GCN1, and (2) increased availability of the GCN2–GCN1 complex enhances sensitivity to uncharged tRNAs.

It is interesting that in yeast, depolymerization of F-actin does not result in a detectable increase in P-eIF2α levels, at least under our experimental conditions. We did not assess directly the autophosphorylation of GCN2, so it is possible that GCN2 is activated but it does not phosphorylate eIF2α. Alternatively, in yeast, actin needs to be fully depolymerized to lead to Gcn2 activation followed by eIF2 phosphorylation. Another scenario is that the signal from the actin cytoskeleton to translation might not be conserved, and it might be more relevant in mammals. However, there is evidence that opposes such a divergent model. Yih1 forms a complex with monomeric-G actin (Sattlegger et al., 2004). Actin haploinsufficient yeast cells are less able to overcome amino acid starvation and this phenotype is partially reverted when *YIH1* is deleted. This supports the idea that under low actin levels, Yih1 is driven to a complex with Gcn1, thus impairing GAAC. Deletion of *Yih1* has no effect on the Gcn2 response, but overexpressed Yih1 strongly inhibits Gcn2. Based on those findings, the proposed model for yeast suggests that Yih1 shuttles from the actin cytoskeleton to Gcn1 to inhibit Gcn2 function, perhaps as a mechanism to enable Yih1-driven localized Gcn2 inhibition (Sattlegger et al., 2004). Thus, we favor an interpretation for our yeast data that increased eIF2α phosphorylation in response to actin depolymerization might be a localized event, not detectable by immunoblots of whole cell extracts.

Taken together, our results show a cross-talk between the cytoskeleton and translation in mammalian cells that is mediated by GCN2. Importantly, these studies demonstrated that the relevant protein interactions can be modified by alterations in the actin cytoskeleton. Dynamic changes of the G-actin:F-actin ratio that occur under physiological conditions might reconfigure the association of GCN2 with its regulators and consequently its activity, potentially allowing for spatiotemporal regulation of protein synthesis.

Our findings underscore the relevance of further investigations on the mechanisms that modulate GCN2 activation and its ability to phosphorylate its substrate eIF2α.

MATERIALS AND METHODS

Cell culture, transfection, and stress conditions

Gcn2$^{+/+}$ and *Gcn2*$^{-/-}$ MEFs were maintained in Dulbecco's Modified Eagle's medium (DMEM), high glucose, supplemented with 10% (v/v) fetal calf serum (FCS) (Gibco), as described (Pereira et al., 2005). Transfection of cells grown to ∼50% confluence with siRNAs was performed using Lipofectamine 2000 (Life Technologies), according to the manufacturer's instructions, for 5 h in Opti-MEM (Life Technologies). A total of 200 pmol of siGCN1 (sense strand): 5′-GCUGGCAUGUGAGCUGGAUAGUUAA-3 (AF232228.1_stealth_3362, Life-Technologies) or of siControl (Stealth RNAi™ siRNA Negative Control, 12935300, Life-Technologies) were used. Opti-MEM was then replaced with fresh DMEM and cells were incubated for 16 h prior to treatments.

Stock solutions of latrunculin-B, cytochalasin-D, jasplakinolide and nocodazole (Sigma-Aldrich) were prepared in DMSO to a final concentration of 1 mg/ml and used at a final concentration of 1 µg/ml in all experiments described. DMSO (0.1%) was included in all control conditions. MEFs were subjected to leucine starvation by culturing in DMEM lacking L-leucine (Emcare, Brazil) supplemented with 10% dialyzed FCS (Gibco). N2a cells were grown and transfected with siIMPACT and siControl (scrambled for siIMPACT) as previously described (Roffe et al., 2013).

Antibodies

Primary antibodies used were: rabbit anti-ThrP^{899}-GCN2 (Abcam, ab75836, 1:1000), rabbit anti-SerP^{52}-eIF2α (Invitrogen, 44-728G, 1:2000), mouse anti-eIF2α (Invitrogen, AHO0802, 1:1000), rabbit anti-CREB2-ATF4 (Santa Cruz, SC200, 1:500), mouse anti-GADD-153/CHOP (Santa Cruz, SC7351, 1:400), mouse anti-actin (Sigma-Aldrich, A1978, 1:4000), rabbit anti-actin (Sigma-Aldrich, A2066, 1:5000), rabbit anti-GAPDH (Sigma-Aldrich, G9545, 1:10,000), rabbit anti-eEF1A (Millipore, 05-235, 1:2000), and mouse anti-puromycin (Millipore, MABE343, clone 12D10, 1:5000). Affinity-purified rabbit anti-GCN1 and anti-IMPACT, guinea pig anti-GCN2 and anti-IMPACT (Pereira et al., 2005), and rabbit serum against *Saccharomyces cerevisiae* eIF2α (Sui2) (Hashimoto et al., 2002) were previously described.

Cell extracts, immunoblots and immunoprecipitations

MEF and N2a cell extracts were prepared in ice-cold immunoprecipitation (IP) lysis buffer as described (Silva et al., 2015). Immunoblots were as described previously (Silva et al., 2015). GCN1 and GCN2 were resolved on 6% gels and all other proteins on 10% gels.

Cell extracts (700 µg for IPs with anti-IMPACT and anti-GCN2 antibodies or 500 µg for IPs with anti-GCN1 and anti-eEF1A antibodies) were pre-cleared with 20 µl of protein-G (for IMPACT and GCN2 IPs) or protein-A (for eEF1A and GCN1 IPs) agarose beads for 1 h at 4°C. Pre-cleared lysates were incubated at 4°C for 2–4 h (for eEF1A IP) or overnight (for IMPACT, GCN1 and GCN2 IPs) with 20 µl of protein A or protein-G agarose beads (Sigma-Aldrich) to which antibodies against eEF1A (500 ng) or GCN1, GCN2 or guinea pig anti-IMPACT (250 ng) had been previously adsorbed. For controls, agarose beads pre-incubated with the same amounts of non-specific antibodies of the same species and isotype were incubated with the same concentration of cell extracts. Beads were washed three times with ice-cold IP buffer and twice with the same buffer without Triton X-100. Beads were resuspended in 20 µl of 1×Laemli's loading buffer (120 mM Tris pH 6.8, 4% SDS, 5% β-mercaptoethanol, 20% glycerol and 0.02% Bromophenol Blue), incubated at 90°C for 2 min, briefly centrifuged and supernatants resolved on SDS-PAGE. Immunoprecipitation of IMPACT–FLAG, expressed in N2a cells differentiated for 64 h (Roffe et al., 2013), was performed as described (Silva et al., 2015).

Flow cytometry analyses

Cells were washed with phosphate-buffered saline (PBS) and trypsinized with 0.25% (v/v) trypsin-EDTA (GIBCO) for 2–5 min at 37°C (5% CO_2). Cells (1×10^6) were harvested by centrifugation at 800 ***g*** for 5 min at room temperature and fixed with 4% (w/v) paraformaldehyde (Electron Microscopy Sciences) in PBS for 1 h. Cells were washed with PBS, permeabilized with 0.1% Triton X-100 and incubated in the dark at room temperature for 30 min with phalloidin–FITC (Sigma-Aldrich) or Alexa-594–DNaseI (Life Technologies) according to the manufacturer's instructions. Cells were washed, resuspended in PBS and fluorescence was quantified in a FACSCanto flow cytometer (BD Bioscience). Unstained cells were used to set the baseline. The average F-actin or G-actin content of a population was expressed as the mean of the fluorescence intensity, as determined with Flowjo software (version, 9.3.3, Tree Star Inc).

Measurement of protein synthesis

Puromycin labeling was performed as previously described (Schmidt et al., 2009). Briefly, MEFs (∼50% confluence) were incubated at 37°C with pre-warmed fresh medium containing 10 µg/ml puromycin (Sigma-Aldrich) for 10 min. Where indicated, cycloheximide (25 µM) (Sigma-Aldrich) was added 5 min before the addition of puromycin. Cells were then washed twice with cold PBS, scraped from the culture dish directly on 4× Laemmli buffer and incubated for 10 min at 80°C under vigorous agitation, and lysates used for immunoblots. The intensity of the chemiluminescence signal was quantified using NIH ImageJ software.

Analysis of tRNA aminoacylation by northern blot

Total RNA was isolated with TRizol® (Thermo Fisher Scientific) according to the manufacturer's instruction, under acidic conditions (pH 4.5). Briefly, cells were directly lysed by adding TRIzol® to culture dishes. The homogenized samples were incubated for 5 min at room temperature and chloroform was then added. Samples were centrifuged at 12,000 ***g*** for 15 min at 4°C. The aqueous layer formed was adjusted to 0.3 M sodium acetate, pH 4.5. RNA was precipitated with isopropanol, washed with 75% ethanol, air-dried at room temperature and resuspended in 5 mM sodium acetate, pH 4.5. As a control, tRNAs were deacylated by adding an equal volume of a 100 mM Tris-HCl, 100 mM NaCl (pH 9.5) solution and incubating samples at 70°C for 30 min. RNA electrophoresis and transfer were performed as described (Jester et al., 2003). Briefly, RNA (45 µg) was resuspended in 1× acidic RNA loading buffer (8 M urea, 0.3 M sodium acetate pH 4.5, 5% glycerol, 0.05% Bromphenol Blue and 0.05% xylene cyanol) and separated by electrophoresis on a 14% polyacrylamide, pH 4.5, 8 M urea gel (50 V at 4°C for ∼20 h) in acidic electrophoresis buffer (0.3 M sodium acetate, pH 4.5). RNA was stained with SYBR Green II (Life Technologies), then electroblotted onto nylon membranes (Hybond-N+, GE Lifescience), followed by crosslinking at 1200 µJoules. Membranes were dried at 50°C for 20 min. Hybridization was performed according to Huang et al. (2014) with some modifications. Membranes were incubated for 4 h at 42°C in hybridization buffer (200 mM Na_2HPO_4, pH 7.0, 0.1% SDS, 10 µg/ml salmon sperm DNA). Hybridization was at 42°C for at least 20 h in the same pre-warmed buffer containing 100 pmol/ml biotin-labeled probe for detection of $tRNA^{Leu}$ (codon CAG): TTAGACCGCTCGGCCATCC-TG. Membranes were washed three times for 5 min with 1× SSC, 0.1% SDS, incubated with hybridization buffer for 30 min and then with fresh hybridization buffer containing streptavidin-HRP conjugate (Sigma-Aldrich) for 30 min at room temperature. After three washes with 1× SSC, 0.1% SDS, tRNAs were detected with Ilumina-Forte substrate (Millipore) using the Alliance 4.7 imaging system (UVITEC Limited, Cambridge, UK).

Yeast methods

Saccharomyces cerevisiae strain H1511 (MATα *ura3*-52 *trp1*-63 *leu2*-3112 *GAL2*+) (Foiani et al., 1991) and its isogenic *gcn2Δ* strain H2557 (Sattlegger and Hinnebusch, 2000) were grown in Synthetic Dextrose medium supplemented with nutritional requirements. For disruption of the cytoskeleton, yeast cells were grown to A_{600nm} of 0.4–0.6 and collected by brief centrifugation. Pre-warmed fresh medium containing 1 µg/ml latrunculin-B or 1 µg/ml nocodazole was added and cells were incubated for the indicated times. To elicit amino acid starvation, 10 mM 3-amino-1,2,4-triazole (3-AT) (Sigma-Aldrich) was added to cells grown in Synthetic Dextrose medium. Cell extracts and immunoblots were as described (Visweswaraiah et al., 2011; Wiedemann et al., 2013). To determine β-galactosidase activity, cells transformed with plasmid p180 (Foiani et al., 1991) were broken in LacZ breaking buffer and enzyme activity measured as described (Yang et al., 2000).

To estimate F-actin content, cells (strain H1511) were harvested at 3000 ***g*** for 3 min at room temperature, washed with PBS, fixed in 3.7% (w/v) formaldehyde (Merck) for 4 h at 4°C, washed and the suspension sonicated for 10 s at setting 30% (1 s on, 1 s off). Cells (∼5×10^6) were permeabilized with 0.1% Triton X-100 for 15 min, washed with PBS, stained with phalloidin–FITC for 1 h at room temperature in the dark and analyzed by flow cytometry as described above.

Acknowledgements

We thank Rafael Calil for help with immunoblots.

Competing interests

The authors declare no competing or financial interests.

Author contributions

R.C.S. designed, performed experiments and interpreted data. E.S. designed experiments and interpreted data. B.A.C. designed experiments and interpreted data. R.C.S., E.S. and B.A.C. wrote the manuscript.

Funding

This work was supported by Fundação de Amparo à Pesquisa do Estado de São Paulo (2009/52047-5 and 2014/23889-6) and Conselho Nacional de Desenvolvimento Científico e Tecnológico (309860/2011-3 and 478903/2012-0) grants to B.A.C.; Health Research Council of New Zealand Emerging Researcher grant, Auckland Medical Research Foundation, Maurice and Phyllis Paykel Trust, and Massey University Research Fund to E.S. R.C.S. was a recipient of a Fundação de Amparo à Pesquisa do Estado de São Paulo/Coordenação de Aperfeiçoamento de Pessoal de Nível Superior postdoctoral fellowship (2014/17145-4).

Supplementary information

Supplementary information available online at
http://jcs.biologists.org/lookup/doi/10.1242/jcs.194738.supplemental

References

Baird, T. D. and Wek, R. C. (2012). Eukaryotic initiation factor 2 phosphorylation and translational control in metabolism. *Adv. Nutr.* **3**, 307-321.
Bektaş, M., Nurten, R., Gürel, Z., Sayers, Z. and Bermek, E. (1994). Interactions of eukaryotic elongation factor 2 with actin: a possible link between protein synthetic machinery and cytoskeleton. *FEBS Lett.* **356**, 89-93.
Bubb, M. R., Senderowicz, A., Sausville, E. A., Duncan, K. and Korn, E. D. (1994). Jasplakinolide, a cytotoxic natural product, induces actin polymerization and competitively inhibits the binding of phalloidin to F-actin. *J. Biol. Chem.* **269**, 14869-14871.
Cambiaghi, T. D., Pereira, C. M., Shanmugam, R., Bolech, M., Wek, R. C., Sattlegger, E. and Castilho, B. A. (2014). Evolutionarily conserved IMPACT impairs various stress responses that require GCN1 for activating the eIF2 kinase GCN2. *Biochem. Biophys. Res. Commun.* **443**, 592-597.
Cameroni, E., De Virgilio, C. and Deloche, O. (2006). Phosphatidylinositol 4-phosphate is required for translation initiation in Saccharomyces cerevisiae. *J. Biol. Chem.* **281**, 38139-38149.
Castilho, B. A., Shanmugam, R., Silva, R. C., Ramesh, R., Himme, B. M. and Sattlegger, E. (2014). Keeping the eIF2 alpha kinase Gcn2 in check. *Biochim. Biophys. Acta* **1843**, 1948-1968.
Chambers, J. E., Dalton, L. E., Clarke, H. J., Malzer, E., Dominicus, C. S., Patel, V., Moorhead, G., Ron, D. and Marciniak, S. J. (2015). Actin dynamics tune the integrated stress response by regulating eukaryotic initiation factor 2α dephosphorylation. *eLife* **4**, e04872.
Chen, R., Rato, C., Yan, Y., Crespillo-Casado, A., Clarke, H. J., Harding, H. P., Marciniak, S. J., Read, R. J. Ron, D. (2015). G-actin provides substrate-specificity to eukaryotic initiation factor 2alpha holophosphatases. *eLife* **4**, e04871.
Dang, C. V., Yang, D. C. and Pollard, T. D. (1983). Association of methionyl-tRNA synthetase with detergent-insoluble components of the rough endoplasmic reticulum. *J. Cell Biol.* **96**, 1138-1147.
Dever, T. E. (2002). Gene-specific regulation by general translation factors. *Cell* **108**, 545-556.
Donnelly, N., Gorman, A. M., Gupta, S. and Samali, A. (2013). The eIF2alpha kinases: their structures and functions. *Cell. Mol. Life Sci.* **70**, 3493-3511.
Edmonds, B. T., Wyckoff, J., Yeung, Y.-G., Wang, Y., Stanley, E. R., Jones, J., Segall, J. and Condeelis, J. (1996). Elongation factor-1 alpha is an overexpressed actin binding protein in metastatic rat mammary adenocarcinoma. *J. Cell Sci.* **109**, 2705-2714.
Foiani, M., Cigan, A. M., Paddon, C. J., Harashima, S. and Hinnebusch, A. G. (1991). GCD2, a translational repressor of the GCN4 gene, has a general function in the initiation of protein synthesis in Saccharomyces cerevisiae. *Mol. Cell. Biol.* **11**, 3203-3216.
Furukawa, R., Jinks, T. M., Tishgarten, T., Mazzawi, M., Morris, D. R. and Fechheimer, M. (2001). Elongation factor 1beta is an actin-binding protein. *Biochim. Biophys. Acta* **1527**, 130-140.
Garcia-Barrio, M., Dong, J., Ufano, S. and Hinnebusch, A. G. (2000). Association of GCN1-GCN20 regulatory complex with the N-terminus of eIF2alpha kinase GCN2 is required for GCN2 activation. *EMBO J.* **19**, 1887-1899.
Garriz, A., Qiu, H., Dey, M., Seo, E.-J., Dever, T. E. and Hinnebusch, A. G. (2009). A network of hydrophobic residues impeding helix alphaC rotation maintains latency of kinase Gcn2, which phosphorylates the alpha subunit of translation initiation factor 2. *Mol. Cell. Biol.* **29**, 1592-1607.
Gross, S. R. and Kinzy, T. G. (2007). Improper organization of the actin cytoskeleton affects protein synthesis at initiation. *Mol. Cell. Biol.* **27**, 1974-1989.
Harding, H. P., Novoa, I., Zhang, Y., Zeng, H., Wek, R., Schapira, M. and Ron, D. (2000). Regulated translation initiation controls stress-induced gene expression in mammalian cells. *Mol. Cell* **6**, 1099-1108.
Hashimoto, N. N., Carnevalli, L. S. and Castilho, B. A. (2002). Translation initiation at non-AUG codons mediated by weakened association of eukaryotic initiation factor (eIF) 2 subunits. *Biochem. J.* **367**, 359-368.
Hinnebusch, A. G. (2005). Translational regulation of GCN4 and the general amino acid control of yeast. *Annu. Rev. Microbiol.* **59**, 407-450.

Hinnebusch, A. G. (2014). The scanning mechanism of eukaryotic translation initiation. *Annu. Rev. Biochem.* **83**, 779-812.
Howe, J. G. and Hershey, J. W. (1984). Translational initiation factor and ribosome association with the cytoskeletal framework fraction from HeLa cells. *Cell* **37**, 85-93.
Huang, Q., Mao, Z. N., Li, S. Q., Hu, J. and Zhu, Y. G. (2014). A non-radioactive method for small RNA detection by northern blotting. *Rice* **7**, 26.
Jester, B. C., Levengood, J. D., Roy, H., Ibba, M. and Devine, K. M. (2003). Nonorthologous replacement of lysyl-tRNA synthetase prevents addition of lysine analogues to the genetic code. *Proc. Natl. Acad. Sci. USA* **100**, 14351-14356.
Kaminska, M., Havrylenko, S., Decottignies, P., Gillet, S., Le Marechal, P., Negrutskii, B. and Mirande, M. (2009). Dissection of the structural organization of the aminoacyl-tRNA synthetase complex. *J. Biol. Chem.* **284**, 6053-6060.
Kandl, K. A., Munshi, R., Ortiz, P. A., Andersen, G. R., Kinzy, T. G. and Adams, A. E. (2002). Identification of a role for actin in translational fidelity in yeast. *Mol. Genet. Genomics* **268**, 10-18.
Kelly, M. T., Yao, Y., Sondhi, R. and Sacktor, T. C. (2007). Actin polymerization regulates the synthesis of PKMzeta in LTP. *Neuropharmacology* **52**, 41-45.
Kim, S. and Coulombe, P. A. (2010). Emerging role for the cytoskeleton as an organizer and regulator of translation. *Nat. Rev. Mol. Cell Biol.* **11**, 75-81.
Lageix, S., Zhang, J., Rothenburg, S. and Hinnebusch, A. G. (2015). Interaction between the tRNA-binding and C-terminal domains of Yeast Gcn2 regulates kinase activity in vivo. *PLoS Genet.* **11**, e1004991.
Liu, G., Tang, J., Edmonds, B. T., Murray, J., Levin, S. and Condeelis, J. (1996). F-actin sequesters elongation factor 1alpha from interaction with aminoacyl-tRNA in a pH-dependent reaction. *J. Cell Biol.* **135**, 953-963.
Liu, G., Grant, W. M., Persky, D., Latham, V. M., Jr, Singer, R. H. and Condeelis, J. (2002). Interactions of elongation factor 1alpha with F-actin and beta-actin mRNA: implications for anchoring mRNA in cell protrusions. *Mol. Biol. Cell* **13**, 579-592.
Marton, M. J., Crouch, D. and Hinnebusch, A. G. (1993). GCN1, a translational activator of GCN4 in Saccharomyces cerevisiae, is required for phosphorylation of eukaryotic translation initiation factor 2 by protein kinase GCN2. *Mol. Cell. Biol.* **13**, 3541-3556.
Marton, M. J., Vazquez de Aldana, C. R., Qiu, H., Chakraburtty, K. and Hinnebusch, A. G. (1997). Evidence that GCN1 and GCN20, translational regulators of GCN4, function on elongating ribosomes in activation of eIF2alpha kinase GCN2. *Mol. Cell. Biol.* **17**, 4474-4489.
Munshi, R., Kandl, K. A., Carr-Schmid, A., Whitacre, J. L., Adams, A. E. and Kinzy, T. G. (2001). Overexpression of translation elongation factor 1A affects the organization and function of the actin cytoskeleton in yeast. *Genetics* **157**, 1425-1436.
Pereira, C. M., Sattlegger, E., Jiang, H.-Y., Longo, B. M., Jaqueta, C. B., Hinnebusch, A. G., Wek, R. C., Mello, L. E. and Castilho, B. A. (2005). IMPACT, a protein preferentially expressed in the mouse brain, binds GCN1 and inhibits GCN2 activation. *J. Biol. Chem.* **280**, 28316-28323.
Perez, W. B. and Kinzy, T. G. (2014). Translation elongation factor 1A mutants with altered actin bundling activity show reduced aminoacyl-tRNA binding and alter initiation via eIF2alpha phosphorylation. *J. Biol. Chem.* **289**, 20928-20938.
Roffe, M., Hajj, G. N., Azevedo, H. F., Alves, V. S. and Castilho, B. A. (2013). IMPACT is a developmentally regulated protein in neurons that opposes the eukaryotic initiation factor 2alpha kinase GCN2 in the modulation of neurite outgrowth. *J. Biol. Chem.* **288**, 10860-10869.
Sattlegger, E. and Hinnebusch, A. G. (2000). Separate domains in GCN1 for binding protein kinase GCN2 and ribosomes are required for GCN2 activation in amino acid-starved cells. *EMBO J.* **19**, 6622-6633.
Sattlegger, E., Swanson, M. J., Ashcraft, E. A., Jennings, J. L., Fekete, R. A., Link, A. J. and Hinnebusch, A. G. (2004). YIH1 is an actin-binding protein that inhibits protein kinase GCN2 and impairs general amino acid control when overexpressed. *J. Biol. Chem.* **279**, 29952-29962.
Sattlegger, E., Barbosa, J. A. R. G., Moraes, M. C. S., Martins, R. M., Hinnebusch, A. G. and Castilho, B. A. (2011). Gcn1 and actin binding to Yih1: implications for activation of the eIF2 kinase GCN2. *J. Biol. Chem.* **286**, 10341-10355.
Sattlegger, E., Chernova, T. A., Gogoi, N. M., Pillai, I. V., Chernoff, Y. O. and Munn, A. L. (2014). Yeast studies reveal moonlighting functions of the ancient actin cytoskeleton. *IUBMB Life* **66**, 538-545.
Schmidt, E. K., Clavarino, G., Ceppi, M. and Pierre, P. (2009). SUnSET, a nonradioactive method to monitor protein synthesis. *Nat. Methods* **6**, 275-277.
Silva, R. C., Dautel, M., Di Genova, B. M., Amberg, D. C., Castilho, B. A. and Sattlegger, E. (2015). The Gcn2 regulator Yih1 interacts with the Cyclin dependent kinase Cdc28 and promotes cell cycle progression through G2/M in budding yeast. *PLoS ONE* **10**, e0131070.
Sonenberg, N. and Hinnebusch, A. G. (2009). Regulation of translation initiation in eukaryotes: mechanisms and biological targets. *Cell* **136**, 731-745.
Sotelo-Silveira, J., Crispino, M., Puppo, A., Sotelo, J. R. and Koenig, E. (2008). Myelinated axons contain beta-actin mRNA and ZBP-1 in periaxoplasmic ribosomal plaques and depend on cyclic AMP and F-actin integrity for in vitro translation. *J. Neurochem.* **104**, 545-557.
Spector, I., Shochet, N. R., Blasberger, D. and Kashman, Y. (1989). Latrunculins-novel marine macrolides that disrupt microfilament organization and affect cell growth: I. Comparison with cytochalasin D. *Cell Motil. Cytoskeleton* **13**, 127-144.
Stapulionis, R., Kolli, S. and Deutscher, M. P. (1997). Efficient mammalian protein synthesis requires an intact F-actin system. *J. Biol. Chem.* **272**, 24980-24986.
Tattoli, I., Sorbara, M. T., Vuckovic, D., Ling, A., Soares, F., Carneiro, L. A. M., Yang, C., Emili, A., Philpott, D. J. and Girardin, S. E. (2012). Amino acid starvation induced by invasive bacterial pathogens triggers an innate host defense program. *Cell Host Microbe* **11**, 563-575.
Vattem, K. M. and Wek, R. C. (2004). Reinitiation involving upstream ORFs regulates ATF4 mRNA translation in mammalian cells. *Proc. Natl. Acad. Sci. USA* **101**, 11269-11274.
Visweswaraiah, J., Lageix, S., Castilho, B. A., Izotova, L., Kinzy, T. G., Hinnebusch, A. G. and Sattlegger, E. (2011). Evidence that eukaryotic translation elongation factor 1A (eEF1A) binds the Gcn2 protein C terminus and inhibits Gcn2 activity. *J. Biol. Chem.* **286**, 36568-36579.
Waller, T., Lee, S. J. and Sattlegger, E. (2012). Evidence that Yih1 resides in a complex with ribosomes. *FEBS J.* **279**, 1761-1776.
Wiedemann, M., Lee, S. J., Silva, R. C., Visweswaraiah, J., Soppert, J. and Sattlegger, E. (2013). Simultaneous semi-dry electrophoretic transfer of a wide range of differently sized proteins for immunoblotting. *Protoc. Exch.*, doi:10.1038/protex.2013.095.
Yang, R., Wek, S. A. and Wek, R. C. (2000). Glucose limitation induces GCN4 translation by activation of Gcn2 protein kinase. *Mol. Cell. Biol.* **20**, 2706-2717.
Young, S. K., Willy, J. A., Wu, C., Sachs, M. S. and Wek, R. C. (2015). Ribosome reinitiation directs gene-specific translation and regulates the integrated stress response. *J. Biol. Chem.* **290**, 28257-28271.